CFD Letters

Journal homepage:
https://semarakilmu.com.my/journals/index.php/CFD_Letters/index
ISSN: 2180-1363

Performance Improvement of a Savonius Wind Turbine using Wavy Concave Blades

Mohanad Al-Ghriybah[1,*], Djamal Hissein Didane[2]

[1] Department of Renewable Energy Engineering, Faculty of Engineering, Isra University, Amman, Jordan
[2] Center for Energy and Industrial Environment Studies, Universiti Tun Hussein Onn Malaysia, Malaysia

ARTICLE INFO

Article history:
Received 6 February 2023
Received in revised form 8 March 2023
Accepted 4 April 2023
Available online 1 September 2023

Keywords:
Savonius; VAWT; blade profile; wavy rotor

ABSTRACT

As the best replacement for fossil fuels, green energy resources have established their significance on a worldwide basis. The availability of wind energy makes it the best promising form of green energy. For transforming wind kinetic energy into mechanical energy at low wind speeds, the Savonius wind rotor is regarded as the best choice. The main goal of the current study is to improve the power coefficient (Cp) and torque coefficient (Ct) of the Conventional Savonius wind turbine (SWT) by modifying the inner surface of the blade using a wavy profile. The aerodynamic performance of the wavy turbine is then compared with the conventional turbine in terms of Cp and Ct. The study is conducted using numerical simulation with the assistance of the ANSYS software. The flow characteristics around the turbines are solved utilizing the SST k-ω turbulence model. The simulation outcomes confirmed that the Cp of the wavy rotor increased by about 14.5% at a tip speed ratio of λ= 0.4. Additionally, outcomes showed the peak Cp is 0.18 at λ=0.7 which is 12.5% greater than the conventional SWT.

1. Introduction

Non-renewable resources including natural gas, coal, and oil have been used up quickly in the last decade as a result of the rapid rise in population numbers and global economic expansion [1]. About 70% of the energy used in the world comes from burning fossil fuels [2, 3]. The burning of these fuels, however, results in the release of greenhouse gases, which are now believed to be the cause of climate change [4, 5]. As a result, people have begun to focus on the use of renewable energy sources like hydropower, wind, biomass, and solar energy. Wind turbines (WTs) are machinery that transforms kinetic energy in the wind into electric power. WTs can be classified into two main groups depending on the direction of their rotation axis: horizontal axis wind turbines (HAWTs) and vertical axis wind turbines (VAWTs) [6]. Because of their easy manufacture, inexpensive price, and low operating noise, VAWTs are widely employed. VAWTs are classified into two main types including Savonius wind turbines (SWTs) and Darrius wind turbines (DWTs). Conventional SWTs are

* *Corresponding author.*
E-mail address: Mohanad.alghriybah@iu.edu.jo (Mohanad Al-Ghriybah)

https://doi.org/10.37934/cfdl.15.9.3244

significantly less effective in the capturing wind than HAWT and DWTs, which severely limits their use and promotion [7].

A lot of research has been done by various researchers to increase the SWT's capacity to capture the wind. The turbine structure's parameters can be changed as one of the upgrades. Structure parameters include Blade overlap ratio (BOR), Aspect ratio (AR), number of stages (NS), number of blades (NB), endplates (EB), and Blade profile (BP).

SWTs with BOR have better efficiency and self-starting ability, because of the enhancement in pressure on blades [8]. Alom *et al.,* [9] conducted a numerical study to examine several elliptical lines with BOR ranging from 0 to 0.3. The results demonstrated that the max Cp occurs at BOR=0.15 with a value of 0.34. Through experimental study, Hassanzadeh *et al.,* [10] demonstrated that a greater Cp may be produced when the tip speed ratio (TSR) = 0.8 and OR=0.2. Utilizing 2D numerical simulation, Akwa *et al.,* [11] and Nasef *et al.,* [12] proved that the best BOR is 0.15. SWT with dual-stage was tested experimentally by Sharma *et al.,* [13]. Results demonstrated that the Cp max was found to be 0.517 at BOR = 0.094.

Determining a suitable AR boosts angular speed and enhances SWT efficiency [14]. Moreover, bigger AR has an impact comparable to that of the turbine's end plates [15]. Despite the advantages a larger AR would provide, most existing SWTs have low AR for structural reasons [16]. Blackwell *et al.,* [17] used an experimental approach to create an evaluation of the AR effect. The authors looked at two bladed SWT with a BOR of 0.15 and ARs of 1.0 and 1.5. The outcomes demonstrated that the Cp of the SWT with greater AR was marginally improved. According to the study of Zhao *et al.,* [18], AR has also been numerically examined using simulations, and the suggested ideal turbine has possibly the greatest AR in the literature, which is equal to 6. Ferrari *et al.,* [19] achieved gains of about 12% in the max Cp by changing the AR value from AR = 0.55 to AR = 1.66.

Kamoji *et al.,* [20] examined the aerodynamic performance of single, dual, and triple stages SWTs. Results showed that triple stages rotors generate fewer variations in torque coefficient (Ct) as compared to those of single and dual stages rotors. Nevertheless, the Cp is falling by rising the NS at the same AR. Hayashi *et al.,* [21] have conducted an experimental investigation on multi-stage SWTs. The results demonstrated that the variation in Ct over the whole cycle of a multi-stage rotor is positive and uniform compared to the conventional SWT with one stage. Several studies [22, 23] have found that dual-stage helical rotors are better able to capture wind than single-stage and triple-stage helical rotors.

The number of blades (NB) refers to the total number of buckets elements that are connected directly to the SWT. As a general observation, a two blades rotor is recommended for ease of construction especially if there are no power augmentation devices [24, 25]. A study by Wenehenubun *et al.,* [26] has been conducted on the effect of NB on the efficiency of the SWT. Results have demonstrated that the rotor with a double blade showed a higher Cp compared to the rotors with three and four blades. Emmanuel and Jun [27] and Morshed *et al.,* [28] conducted a numerical study on the evolution of the wind flow and pressure distribution nearby rotors with three and six blades, which provides insight into how the loads on the turbine will behave as a function of NB. Though the majority of studies on the impact of NB have used the same geometry for all of the blades, other designs that analyze rotors with multiple inner blades have used designs where not all of the blades are equal [29–32].

Endplates (EB) can be used to increase the Cp of SWT by a significant amount. Endplates keep air from escaping to the atmosphere from the tips of the concave sides of the moving and returning blades. This causes a significant increase in the amount of energy extracted from the wind due to the high-pressure change between the two sides of the blades. According to researchers [33–35] the addition of EB increased SWT's aerodynamic performance by around 11%–36%. This successfully

increased SWT's capacity for self-starting. Sanusi *et al.,* [36] conducted research on the application of EB in the enhanced geometry of an elliptical SWT. The turbine design that was suggested combined a blade with a semicircular shape with an elliptical shape on the concave side. For a TSR of 0.8, the combined blade raised Cp to 0.27. The energy-capturing point was pushed farther from the center of rotation as a result of the employment of an elliptical profile on the concave side, which enhanced the net positive torque operating on the turbine.

Blades are considered one of the main components of SWT. Modifying their profile would influence the captured energy from the rotor. Tian *et al.,* [37] presented a form of blades having various convex and concave sides, using two design variables to reflect the two sides' heights, respectively. The best design parameters were then obtained using particle swarm optimization and a kriging surrogate model. Chan *et al.,* [38] utilized genetic algorithms to find the ideal blade shape while controlling the geometry of the blade using 3 changeable points. Bach-type rotor profiles were enhanced by Roy and Saha [39]. According to the results, the enhanced Bach-type rotor performed 34.8% better than the conventional SWT. In order to acquire the best conetet efigturation for the wind rotor, Mohamed *et al.,* [40] installed a barrier plate in the opposite direction of the SWT and improved the BP. Al-Ghriybah [41] improved the Cp of the SWT by changing the blade thickness utilizing the simulation method. Results demonstrated that the maximum achieved Cp was 0.2 which is 40% more than the conventional SWT.

The aforementioned studies demonstrate that one key strategy for increasing the Savonius wind turbine's ability to capture more energy is by adjusting the blade's profile. However, at present, there is no study that considers using a wavy blade profile which is expected to enhance the surface area of the turbine and hence enhance the extracted power from the SWT. Based on that, this study proposes a wavy shape for the inner surface (concave side) of the SWT.

2. Geometry Description

2.1 Proposed SWT

This study proposes a novel SWT with wavy concave blades. Figure 1 demonstrates the geometrical design of the conventional SWT and the proposed wavy rotor. The main geometrical dimensions are kept the same for both configurations as follows: the diameter of the rotor (Dr) is equal to 0.442 m, the shaft diameter is equal to 0.03 m, and the blade diameter is set to 0.144 m. However, the concave side of the novel rotor has a wavy shape with a dimension of (height = 0.0036m and width = 0.0043).

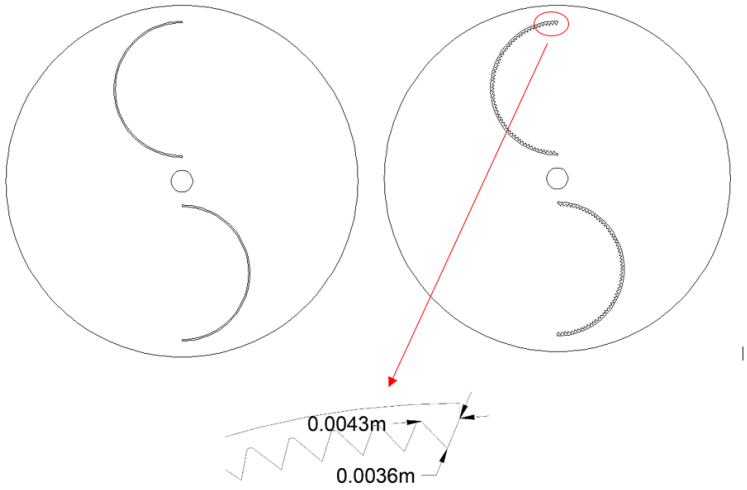

Fig. 1. Conventional SWT vs. wavy SWT

2.2 Performance of SWT

Tip speed ratio (λ) which represents the ratio between the speed of the blade tip (v_{tip}) and prevailing wind speed (U) and is expressed as below [42]:

$$\lambda = \frac{v_{tip}}{U} = \frac{\omega * r}{U} \tag{1}$$

where ω represents the tip angular velocity in rad/s and r embodies the radius of the SWT. With respect to λ, the efficiency of the SWT can be described by two main performance indicators: Cp and Ct. The percentage of airflow that travels over the swept area of SWT (A) in the same path of the wind is represented by Cp. Cp and Ct are expressed using the following expressions:

$$Cp = \frac{P_{out}}{P_{in}} = \frac{P_{out}}{0.5\rho U^3 A} \tag{2}$$

$$Ct = \frac{T_{out}}{T_{in}} = \frac{T_{out}}{0.5\rho U^2 Ar} \tag{3}$$

where P_{out} denotes the output power of the turbine, P_{in} denotes the available power in the wind, and ρ represents the airstream density. T_{out} demonstrates the output torque from the turbine, T_{in} demonstrates the input torque to the turbine. Cp and Ct can be related together based on λ as below:

$$Cp = \lambda * \mathrm{Ct} \tag{4}$$

3. Numerical Modeling

Numerical analysis has been conducted on the conventional and the wavy SWTs using the software “ANSYS Fluent”. Two-dimensional simulation (2D) has been adopted in this study. The 2D simulation has been effectively confirmed to have high accuracy [43, 44]. A series of transient simulations have been implemented to determine the efficiency of the rotors at different values of λ.

3.1 Numerical Domain

Figure 2 illustrates the adopted numerical domain. As shown in the figure, the domain consists mainly of two sub-domains: a revolving circular domain and a fixed rectangular domain. The revolving domain represents the position where the SWT will be placed whereas the fixed domain represents the wind tunnel where the wind will flow. The circular domain has a rotational speed of ω as input since the sliding mesh technique is implemented in the simulation. An interface has been defined between the two sub-domains in order to ensure smooth airflow to the turbine. The long boundaries of the domain (up and down) are set as walls. The left and right boundaries are set as velocity inlet and pressure outlet, respectively. The numerical domain is selected to have a size large enough to prevent boundary effects on the simulation results. According to recommendations made in some literature [45, 46], the top and bottom walls of the numerical domain are determined to be 14×D apart from the center of the circular sub-domain, and the total length of the top and bottom walls is 30×D, the inlet is 14×D upstream of the circular domain center, and the outlet is 26D downstream of the circular sub-domain center. The rotating domain's diameter is fixed at 1.2×D. A no-slip condition

was set on the surfaces of the advancing and returning blades. A 9m/s was set as inlet velocity. The λ was set to different values (0.4, 0.5, 0.6, 0.7) in order to rotate the circular sub-domain with different angular velocities.

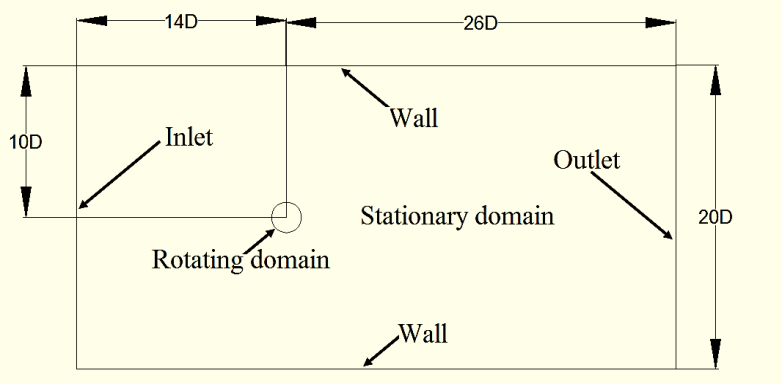

Fig. 2. Numerical domain

3.2 Grid Generation

The mesh of the numerical domain was produced using the built-in software mechanical mesh. The grids of the circular sub-domain should be denser than the rectangular sub-domain in order to obtain accurate results around the rotor. A quadrilateral grid-based, unstructured mesh was generated for both sub-domains. Additionally, the inflation option was activated around the blades (25 layers with a 1.1 growth ratio) in order to capture the airflow around the rotor with high accuracy. Aiming to improve the SWT geometry adaption, a grade 3 refinement was performed to the contact region between the two sub-domains. The final implemented mesh of the domains including the two sub-domains and the inflation layers around the rotor is presented in Figure 3.

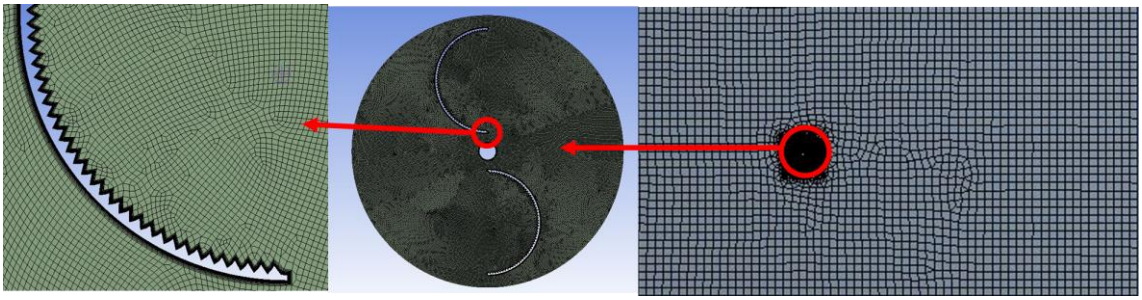

Fig. 3. Grids of the different sub-domains

3.3 Computational Solver Settings

As a result of the transient nature of the wind flow interaction with the rotating blades, flow around the SWT was analyzed utilizing an unsteady solver. The Navier-Stokes equations were solved by the SST k-ω turbulence model. The SST k-ω model has been used extensively in the field of wind turbines and is better suited than other models for estimating the values of the wall friction coefficient [47]. The solver's settings were set as transient. For the pressure and velocity coupling, the SIMPLE algorithm was applied. The sliding mesh technique was utilized to represent the turbine's rotation. The rotor was rotated ten times, each time increasing the azimuth angle by one degree. There were 3600-time steps in all. For each time step, a total of 20 iterations were carried out to guarantee that the residuals were sufficiently small.

4. Results

4.1 Grid Independence Test

A grid independence test (GIT) should be performed in order to determine the best mesh size in order to decrease the computing time and cost without compromising the accuracy of the findings. A GIT has therefore been carried out utilizing an unstructured mesh with six distinct mesh resolutions for the conventional SWT at $\lambda = 0.4$, as illustrated in Figure 4. It is seen from Figure 4 that there is a slight difference in the Cp value while raising the grids over 188,874. Consequently, Mesh 4 with 188,874 elements has been implemented for all further analysis to minimize the cost of the high computations.

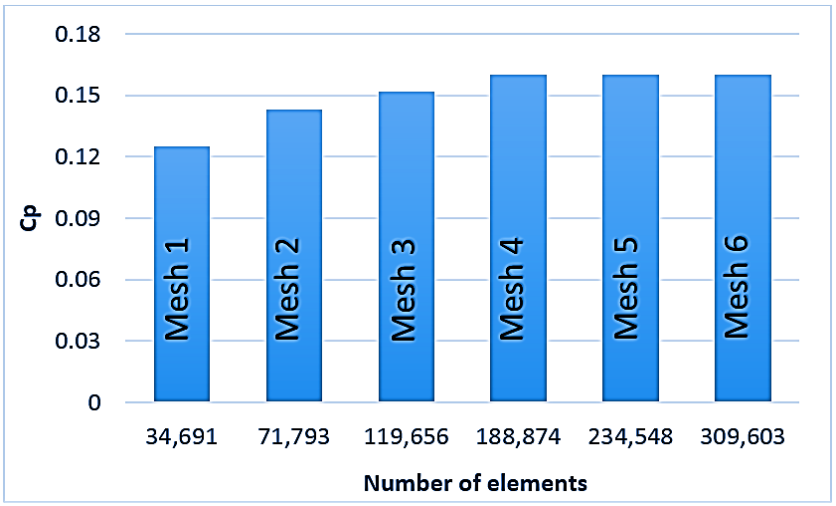

Fig. 4. GIT using a different grid size

4.2 Validation of the Numerical Model

The simulation procedure required to be examined to confirm the validity of the used methodology before moving on to the outcomes of the current study. Since there are no experimental data for the SWT under investigation in this research, Alom and Saha's experimental work [46] was used to validate the turbine's aerodynamic characteristics. The validation has been demonstrated using the Cp from experimental and simulated SWTs. With an overall error of roughly 4.2%, Figure 5 illustrates the near results between the experimental records and the records from the simulation. As a result, the precision of the existing simulation method has been verified to be trustworthy and may be taken into consideration for future simulation operations.

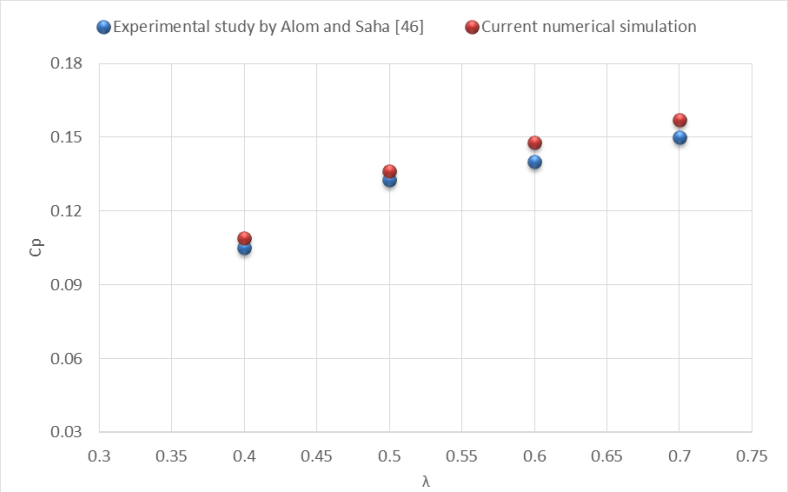

Fig. 5. Validation of the simulation procedure

4.3 Performance Analysis of Cp and Ct

Cp and Ct values are numerically estimated by the simulations for conventional SWT and wavy SWT over the same range of λ (0.4, 0.5, 0.6, and 0.7). Figure 6 demonstrates a Cp comparison between the conventional and wavy SWTs depending on the achieved results from the numerical simulation. It can be noticed from Figure 6 that the wavy SWT has a greater Cp than the conventional Savonius at all the range of λ. The max Cp is observed to be about 0.18 at λ = 0.4 whereas the Cp of the conventional Savonius is observed to be 0.16 at the same point of λ = 0.4. This includes a performance enhancement of about 12.5% compared to the conventional rotor. The maximum improvement can be noticed at λ = 0.4 with a value of 14.5%. This improvement can be attributed to the increase of the inner surface area of the blade due to the inner wavy shape. Increasing the surface area of the blade enhances the amount of the captured energy and hence enhances the performance of the rotor.

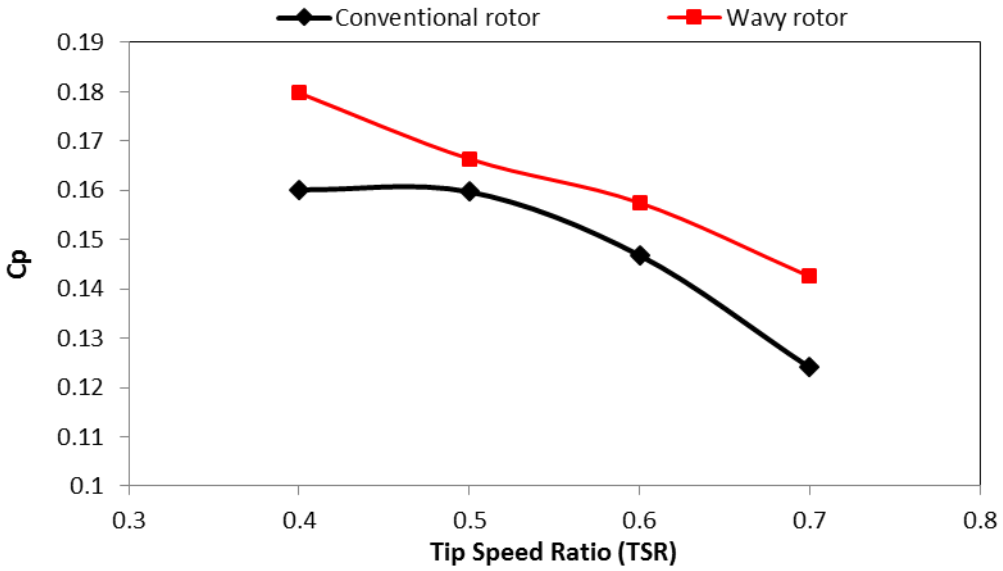

Fig. 6. Comparison of Cp between conventional and wavy SWTs

Figure 7 demonstrates the Ct evaluation for both the conventional and the wavy SWTs at different values of λ. In general, it is observed that adding loads causes the rotors' rotational speed to

decrease; as a result, Ct values decrease as λ values rise. Moreover, it can be realized from Figure 7 that Ct has a peak value of 0.45 at λ = 0.4 whereas at the same value of λ the Ct of the conventional rotor was 0.4. The generated Ct at each angle of rotation (during 360°) is estimated and shown in Figure 8 at λ = 0.7. It is evident from the figure that the generated Ct has two cycles in every rotation. However, the generated torque in the second cycle is less than that in the first cycle. This is due to the wake generated from the rotating of the first advancing blade. Moreover, the peak value of Ct for the wavy rotor is observed to be at the angle of rotation of 120° with a value of 0.725 which is 74% higher than the conventional rotor at the same angle. Moreover, the starting torque at 0° angle of rotation has been improved in the case of a wavy rotor compared to the conventional Savonius. Additionally, it can be observed from figure 8 that the negative Ct has been reduced in the interval between 170°–220° angles of rotation. These observations explain the performance gain of the wavy SWT.

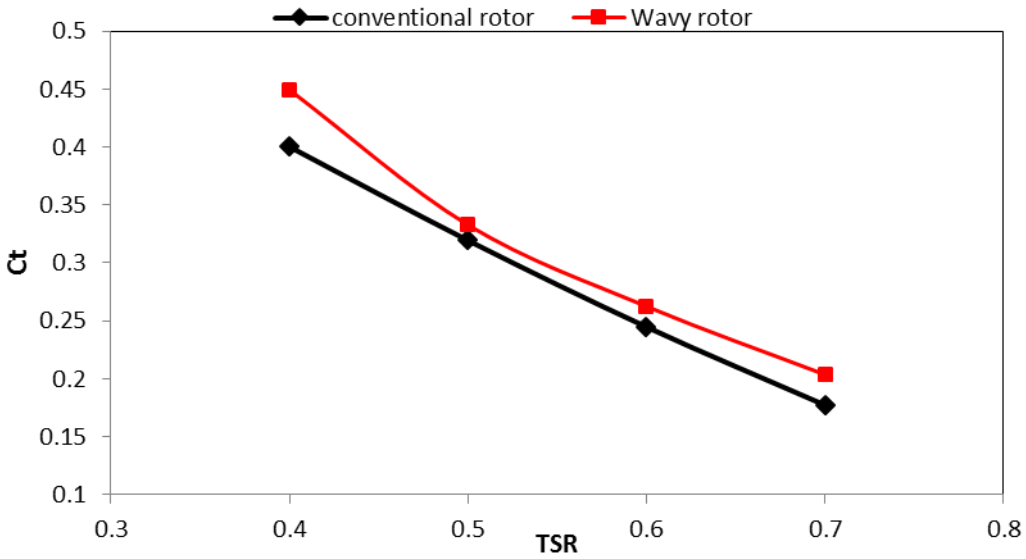

Fig. 7. Comparison of Ct between conventional and wavy SWTs

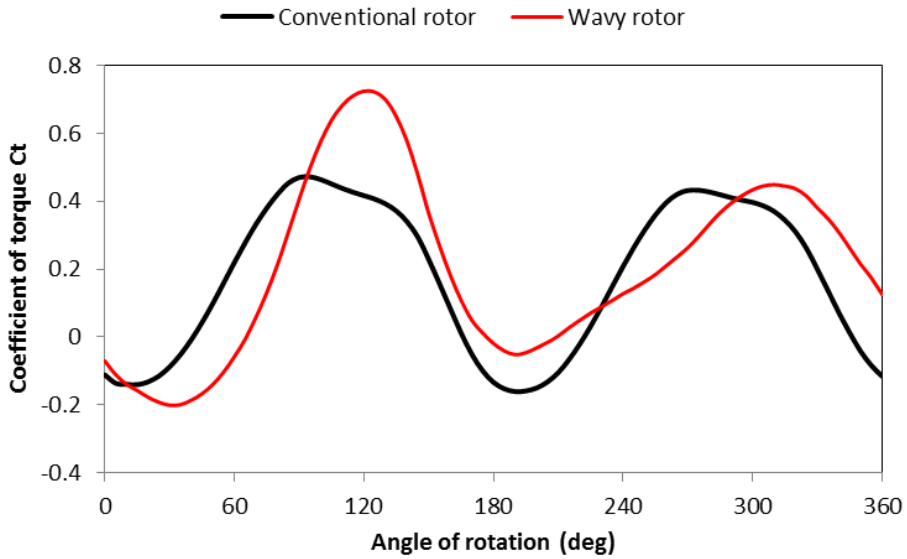

Fig. 8. Generated Ct at each angle of rotation

4.4 Prediction of the Flow Field around the Tested SWTs

The flow characteristic such as pressure distribution contours, velocity distribution contours, and streamlines are shown around the conventional and wavy SWTs. All contours are generated at λ = 0.7 and 120° angle of rotation. In order to better understand the flow properties, pressure distributions of the airflow around the rotors are provided in Figure 9. For the advancing blade, it can be observed from Figure 9 that the concave side has high-pressure regions whereas the convex side has lower-pressure regions. Due to the pressure differences on both sides, the rotor is driven by a strong positive torque. A notable low-pressure region can be seen outside the blade (convex side) and close to the tip of the blade, which causes in rising the driving torque for the wavy SWT compared to the conventional one. During the "returning" process, the blade produces negative torque; in this area, positive pressure operates on the convex side, and negative pressure acts on the opposite side. The net pressure produces a negative torque that prevents the blade from rotating. On the other hand, in comparison to the conventional SWT, the pressure on the convex side of the returning blade for the wavy SWT is lower. By reducing wind resistance on the back side of the returning blade, which will result in a greater positive net drag, this low pressure helps to reduce the negative drag.

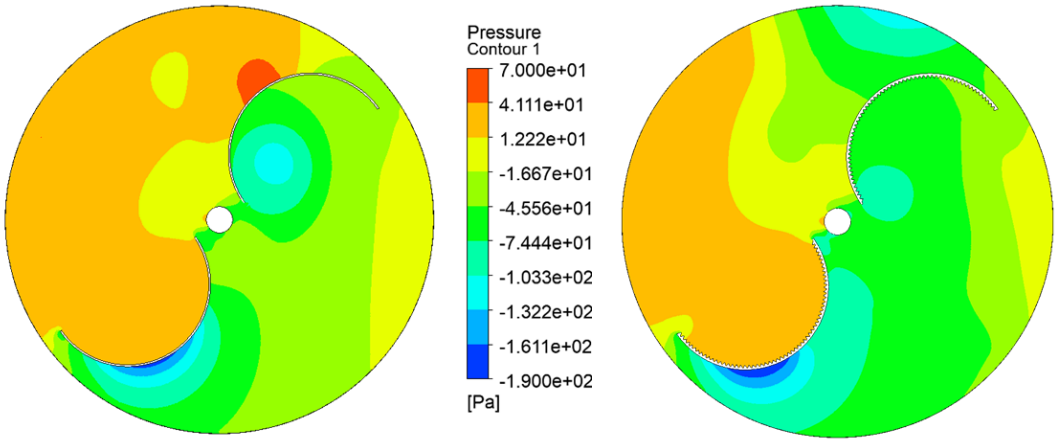

Fig. 9. Pressure distribution around (a) conventional SWT (b) Wavy SWT

Analysis of velocity is essential to gain more understanding of how the rotor's flow develops with the greatest possible improvement (Figure 10). Rotors start spinning as a result of the wind entering from the left boundary (inlet side), which causes the air to travel in a circular pattern all around it. As a result of the air moving in a circular pattern around the rotors, the back side of the returning blade is less affected by the velocity of the incoming air, which reduces the resistance between the surface of the blade and the incoming flow. Because the Wavy SWT has greater tip vortices and recovery Flow, the pressure on the advancing blade's back side is reduced. It happens as a result of the wavy rotor's stronger reverse flow, higher blade-tip velocities, and stronger tip vortices. Additionally, the wavy surface is easier for air to flow along, which causes a faster recovery flow.

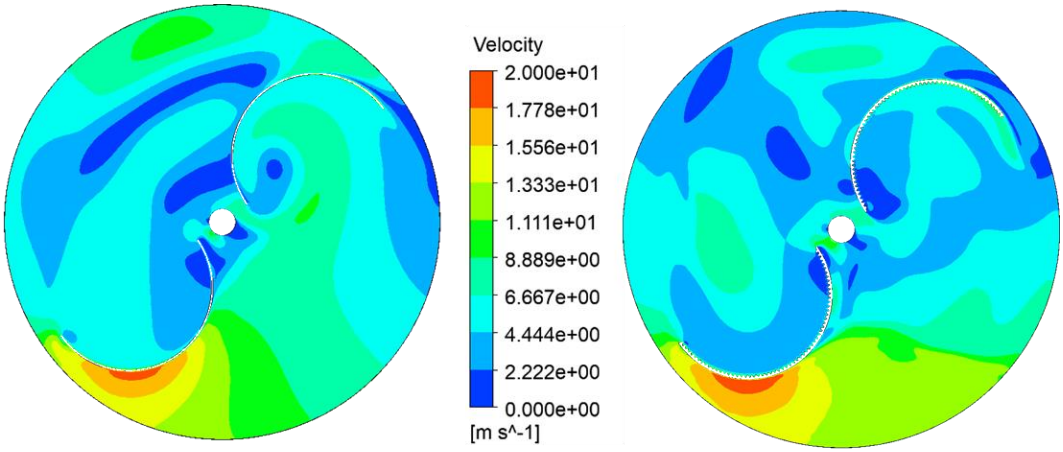

Fig. 10. Velocity distribution around (a) conventional SWT (b) Wavy SWT

The airflow field nearby the conventional and wavy SWTs is investigated based on the generated streamlines. The streamlines for both configurations are presented in Figure 11 at $\lambda = 0.7$, as the vortices can be observed in the surrounding of the turbine. Vortices have been observed near the lower edge and back side of the returning blade. Furthermore, the high-generated vortices behind the returning blade may be seen in contrast to the low-generated vortex in the conventional SWT. These vortices provide additional proof that the wavy rotor's pressure differential is greater than the conventional one, which reduces the impact of entering air on the returning blade and, consequently, the resistance of the returning blade's surface to the wind flow.

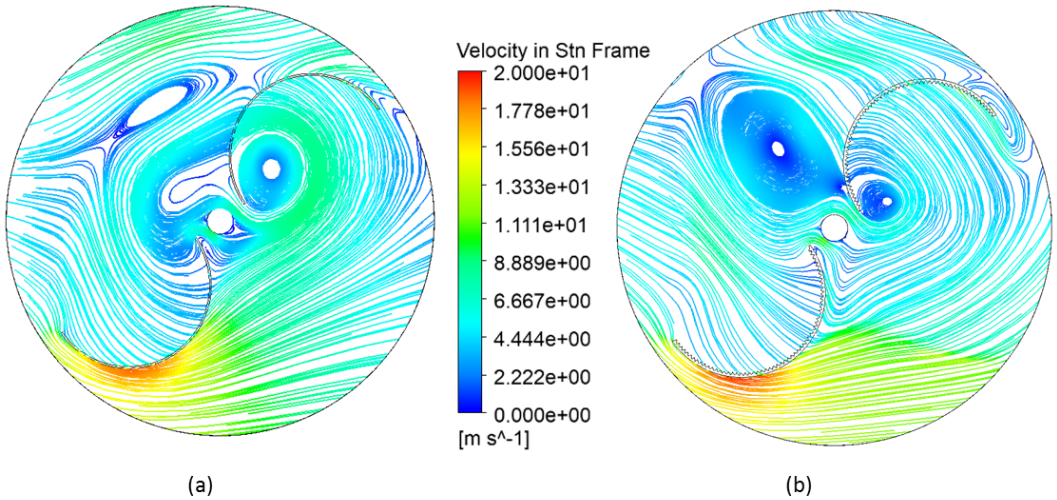

Fig. 11. Streamlines around (a) conventional SWT (b) Wavy SWT

5. Conclusions

In this work, the authors numerically analyzed the impact of modifying the concave side of the blades using a wavy shape. Afterward, the investigation focused on a comparison of the numerical outcomes found for the wavy SWT compared to the conventional SWT. Results demonstrated that both Conventional and wavy SWTs attain maximum power at $\lambda = 0.4$. In terms of the power coefficient (Cp), the wavy geometry shows improved power characteristics than the conventional rotor. The max Cp is observed to be about 0.18 at $\lambda = 0.4$ whereas the Cp of the conventional rotor is

observed to be 0.16 at the same point of λ = 0.4. Additionally, the maximum Ct for the wavy rotor is found to be at the angle of rotation of 120° with a value of Ct = 0.725 which is 74% higher than the conventional rotor at the same angle. The wavy shape is found to have the ability to lower the pressure from the convex side and near the blade tip which leads to an increase in the net-generated torque. The current study shows that significant Savonius rotor power generation improvements can be made without raising manufacturing costs or complicating the design. This approach may be helpful for producing electricity in rural areas more cheaply and efficiently.

Acknowledgement
Communication of this research is made possible through monetary assistance by Universiti Tun Hussein Onn Malaysia and the UTHM Publisher's Office via Publication Fund E15216.

References

[1] Yu, Chenyang, Massoud Moslehpour, Trung Kien Tran, Lam Minh Trung, Jenho Peter Ou, and Nguyen Hoang Tien. "Impact of non-renewable energy and natural resources on economic recovery: Empirical evidence from selected developing economies." *Resources Policy* 80 (2023): 103221. https://doi.org/10.1016/j.resourpol.2022.103221

[2] Lagum, Abdelmajeed Adam. "Simultaneous nitrification and denitrification by controlling current density and dissolved oxygen supply in a novel electrically-induced membrane bioreactor." *Journal of Environmental Management* 322 (2022): 116131. https://doi.org/10.1016/j.jenvman.2022.116131

[3] Mamat, Mohd Nadzri, and Dahaman Ishak. "Analysis of SEPIC-Boost Converter Using Several PID Feedback Tuning Methods for Renewable Energy Applications." *Journal of Advanced Research in Applied Sciences and Engineering Technology* 26, no. 1 (2022): 105-117. https://doi.org/10.37934/araset.26.1.105117

[4] Lagum, Abdelmajeed Adam, and Maria Elektorowicz. "Modification of nitrifying microbial community via DC electrical field application." *Journal of Environmental Chemical Engineering* 10, no. 3 (2022): 107743. https://doi.org/10.1016/j.jece.2022.107743

[5] Rahman, Md Mizanur, Mohd Faizal Hasan, Aminuddin Saat, and Mazlan Abd Wahid. "Renewable Resource based Decentralized Power System to a Remote Village in Malaysia: Optimization and Technoeconomic Evaluation." *Journal of Advanced Research in Fluid Mechanics and Thermal Sciences* 37, no. 1 (2017): 1-17.

[6] Elgendi, Mahmoud, Maryam AlMallahi, Ashraf Abdelkhalig, and Mohamed YE Selim. "A Review of Wind Turbines in Complex Terrain." *International Journal of Thermofluids* (2023): 100289. https://doi.org/10.1016/j.ijft.2023.100289

[7] Patel, Ravi, and Vimal Patel. "Effect of waves on leading edge of modified Savonius rotor blades." *Ocean Engineering* 271 (2023): 113445. https://doi.org/10.1016/j.oceaneng.2022.113445

[8] Brusca, S., A. Galvagno, R. Lanzafame, S. Mauro, and M. Messina. "How to Increase Savonius Power Coefficient: Ducted Rotor Performance with Different Overlap Ratios." *In Journal of Physics: Conference Series* 2385, no. 1, (2022): 012105. https://doi.org/10.1088/1742-6596/2385/1/012105

[9] Alom, Nur, and Ujjwal K. Saha. "Arriving at the optimum overlap ratio for an elliptical-bladed Savonius rotor." *In Turbo Expo: Power for Land, Sea, and Air* 50961, *p. V009T49A012. American Society of Mechanical Engineers,* (2017). https://doi.org/10.1115/GT2017-64137

[10] Hassanzadeh, Rahim, and Milad Mohammadnejad. "Effects of inward and outward overlap ratios on the two-blade Savonius type of vertical axis wind turbine performance." *International Journal of Green Energy* 16, no. 15 (2019): 1485-1496. https://doi.org/10.1080/15435075.2019.1671420

[11] Akwa, João Vicente, Gilmar Alves da Silva Júnior, and Adriane Prisco Petry. "Discussion on the verification of the overlap ratio influence on performance coefficients of a Savonius wind rotor using computational fluid dynamics." *Renewable energy* 38, no. 1 (2012): 141-149. https://doi.org/10.1016/j.renene.2011.07.013

[12] Nasef, M. H., W. A. El-Askary, A. A. Abdel-Hamid, and H. E. Gad. "Evaluation of Savonius rotor performance: Static and dynamic studies." *Journal of Wind Engineering and Industrial Aerodynamics* 123 (2013): 1-11. https://doi.org/10.1016/j.jweia.2013.09.009

[13] Sharma, Kaushal Kumar, Rajat Gupta, and Agnimitra Biswas. "Performance measurement of a two-stage two-bladed Savonius rotor." *International journal of renewable energy research* 4, no. 1 (2014): 115-121. https://doi.org/10.20508/ijrer.v4i1.1028.g6254

[14] Cuevas-Carvajal, N., J. S. Cortes-Ramirez, Julian A. Norato, C. Hernandez, and M. F. Montoya-Vallejo. "Effect of geometrical parameters on the performance of conventional Savonius VAWT: A review." *Renewable and Sustainable Energy Reviews* 161 (2022): 112314. https://doi.org/10.1016/j.rser.2022.112314

[15] Al Noman, Abdullah, Zinat Tasneem, Md Fahad Sahed, S. M. Muyeen, Sajal K. Das, and Firoz Alam. "Towards next generation Savonius wind turbine: Artificial intelligence in blade design trends and framework." *Renewable and Sustainable Energy Reviews* 168 (2022): 112531. https://doi.org/10.1016/j.rser.2022.112531
[16] Dewan, Anupam, Adesh Gautam, and Rahul Goyal. "Savonius wind turbines: A review of recent advances in design and performance enhancements." *Materials Today: Proceedings* 47 (2021): 2976-2983. https://doi.org/10.1016/j.matpr.2021.05.205
[17] Sheldahl, Robert E., Bennie F. Blackwell, and Louis V. Feltz. "Wind tunnel performance data for two-and three-bucket Savonius rotors." *Journal of Energy* 2, no. 3 (1978): 160-164. https://doi.org/10.2514/3.47966
[18] Zhao, Zhenzhou, Yuan Zheng, Xiaoyun Xu, Wenming Liu, and Daqing Zhou. "Optimum design configuration of helical Savonius rotor via numerical study." *In Fluids Engineering Division Summer Meeting* 43727, (2009): 1273-1278. https://doi.org/10.1115/FEDSM2009-78430
[19] Ferrari, G., D. Federici, Paolo Schito, Fabio Inzoli, and Riccardo Mereu. "CFD study of Savonius wind turbine: 3D model validation and parametric analysis." *Renewable energy* 105 (2017): 722-734. https://doi.org/10.1016/j.renene.2016.12.077
[20] Kamoji, M. A., S. B. Kedare, and S. V. Prabhu. "Experimental investigations on single stage, two stage and three stage conventional Savonius rotor." *International journal of energy research* 32, no. 10 (2008): 877-895. https://doi.org/10.1002/er.1399
[21] Hayashi, Tsutomu, Yan Li, and Yutaka Hara. "Wind tunnel tests on a different phase three-stage Savonius rotor." *JSME International Journal Series B Fluids and Thermal Engineering* 48, no. 1 (2005): 9-16. https://doi.org/10.1299/jsmeb.48.9
[22] Frikha, Sobhi, Zied Driss, Emna Ayadi, Zied Masmoudi, and Mohamed Salah Abid. "Numerical and experimental characterization of multi-stage Savonius rotors." *Energy* 114 (2016): 382-404. https://doi.org/10.1016/j.energy.2016.08.017
[23] Saad, Ahmed S., Shinichi Ookawara, and Mahmoud Ahmed. "Influence of varying the stage aspect ratio on the performance of multi-stage Savonius wind rotors." *Journal of Energy Resources Technology* 144, no. 1 (2022). https://doi.org/10.1115/1.4050876
[24] Al-Ghriybah, Mohanad, Mohd Fadhli Zulkafli, Djamal Hissein Didane, and Sofian Mohd. "Review of the recent power augmentation techniques for the Savonius wind turbines." *Journal of Advanced Research in Fluid Mechanics and Thermal Sciences* 60, no. 1 (2019): 71-84.
[25] Shende, Vikas, Harsh Patidar, Prashant Baredar, and Meena Agrawal. "A review on comparative study of Savonius wind turbine rotor performance parameters." *Environmental Science and Pollution Research* 29, no. 46 (2022): 69176-69196. https://doi.org/10.1007/s11356-022-22399-w
[26] Wenehenubun, Frederikus, Andy Saputra, and Hadi Sutanto. "An experimental study on the performance of Savonius wind turbines related with the number of blades." *Energy procedia* 68 (2015): 297-304. https://doi.org/10.1016/j.egypro.2015.03.259
[27] Emmanuel, Binyet, and Wang Jun. "Numerical study of a six-bladed Savonius wind turbine." *Journal of Solar Energy Engineering* 133, no. 4 (2011). https://doi.org/10.1115/1.4004549
[28] Morshed, Khandakar Niaz, Mosfequr Rahman, Gustavo Molina, and Mahbub Ahmed. "Wind tunnel testing and numerical simulation on aerodynamic performance of a three-bladed Savonius wind turbine." *International Journal of Energy and Environmental Engineering* 4 (2013): 1-14. https://doi.org/10.1186/2251-6832-4-18
[29] Al-Ghriybah, Mohanad, Mohd Fadhli Zulkafli, Djamal Hissein Didane, and Sofian Mohd. "Performance of Double Blade Savonius Rotor at Low Rotational Speed." *Journal of Computational and Theoretical Nanoscience* 17, no. 2-3 (2020): 729-735. https://doi.org/10.1166/jctn.2020.8711
[30] Al-Ghriybah, Mohanad, Mohd Fadhli Zulkafli, Djamal Hissein Didane, and Sofian Mohd. "The effect of spacing between inner blades on the performance of the Savonius wind turbine." *Sustainable Energy Technologies and Assessments* 43 (2021): 100988. https://doi.org/10.1016/j.seta.2020.100988
[31] Al-Ghriybah, Mohanad, Mohd Fadhli Zulkafli, Djamal Hissein Didane, and Sofian Mohd. "The effect of inner blade position on the performance of the Savonius rotor." *Sustainable Energy Technologies and Assessments* 36 (2019): 100534. https://doi.org/10.1016/j.seta.2019.100534
[32] Al-Ghriybah, Mohanad, Mohd Fadhli Zulkafli, Djamal Hissein Didane, and Sofian Mohd. "Performance of the Savonius Wind Rotor with Two Inner Blades at Low Tip Speed Ratio." *CFD Letters* 12, no. 3 (2020): 11-21. https://doi.org/10.37934/cfdl.12.3.1121
[33] Alom, Nur, Nitish Kumar, and Ujjwal K. Saha. "Analyzing the effect of shaft and end-plates of a newly developed elliptical-bladed savonius rotor from wind tunnel tests." *In International Conference on Offshore Mechanics and Arctic Engineering, vol. 58899, p. V010T09A049. American Society of Mechanical Engineers,* (2019). https://doi.org/10.1115/OMAE2019-95570
[34] Jeon, Keum Soo, Jun Ik Jeong, Jae-Kyung Pan, and Ki-Wahn Ryu. "Effects of end plates with various shapes and sizes

on helical Savonius wind turbines." *Renewable energy* 79 (2015): 167-176. https://doi.org/10.1016/j.renene.2014.11.035

[35] Saad, Ahmed S., Ibrahim I. El-Sharkawy, Shinichi Ookawara, and Mahmoud Ahmed. "Performance enhancement of twisted-bladed Savonius vertical axis wind turbines." *Energy Conversion and Management* 209 (2020): 112673. https://doi.org/10.1016/j.enconman.2020.112673

[36] Sanusi, Arifin, Sudjito Soeparman, Slamet Wahyudi, and Lilis Yuliati. "Experimental study of combined blade Savonius wind turbine." *International Journal of Renewable Energy Research (IJRER)* 6, no. 2 (2016): 614-619.

[37] Tian, Wenlong, Zhaoyong Mao, Baoshou Zhang, and Yanjun Li. "Shape optimization of a Savonius wind rotor with different convex and concave sides." *Renewable energy* 117 (2018): 287-299. https://doi.org/10.1016/j.renene.2017.10.067

[38] Chan, Chun Man, H. L. Bai, and D. Q. He. "Blade shape optimization of the Savonius wind turbine using a genetic algorithm." *Applied energy* 213 (2018): 148-157. https://doi.org/10.1016/j.apenergy.2018.01.029

[39] Roy, Sukanta, and Ujjwal K. Saha. "Wind tunnel experiments of a newly developed two-bladed Savonius-style wind turbine." *Applied Energy* 137 (2015): 117-125. https://doi.org/10.1016/j.apenergy.2014.10.022

[40] Mohamed, M. H., G. Janiga, E. Pap, and D. Thévenin. "Optimal blade shape of a modified Savonius turbine using an obstacle shielding the returning blade." *Energy Conversion and Management* 52, no. 1 (2011): 236-242. https://doi.org/10.1016/j.enconman.2010.06.070

[41] Al-Ghriybah, Mohanad. "Performance Analysis of a Modified Savonius Rotor Using a Variable Blade Thickness." *EVERGREEN Joint Journal of Novel Carbon Resource Sciences & Green Asia Strategy* (2022): 645-653. https://doi.org/10.5109/4842522

[42] Al-Ghriybah, Mohanad, Mohd F. Zulkafli, and Djamal H. Didane. "Numerical investigation of inner blade effects on the conventional savonius rotor with external overlap." *Journal of Sustainable Development of Energy, Water and Environment Systems* 8, no. 3 (2020): 561-576. https://doi.org/10.13044/j.sdewes.d7.0292

[43] Tian, Wenlong, Baowei Song, James H. VanZwieten, and Parakram Pyakurel. "Computational fluid dynamics prediction of a modified Savonius wind turbine with novel blade shapes." *Energies* 8, no. 8 (2015): 7915-7929. https://doi.org/10.3390/en8087915

[44] Fetalver, Charmaine F., and Christian M. Mortel. "Numerical simulation of two-dimensional (2D) elliptical shape Savonius wind turbine (SWT) blade using response surface methodology." *In AIP Conference Proceedings* 2534, no. 1, (2022): 020002. https://doi.org/10.1063/5.0105197

[45] Alom, Nur, Ujjwal K. Saha, and Anupam Dewan. "In the quest of an appropriate turbulence model for analyzing the aerodynamics of a conventional Savonius (S-type) wind rotor." *Journal of Renewable and Sustainable Energy* 13, no. 2 (2021): 023313. https://doi.org/10.1063/5.0034362

[46] Alom, Nur, and Ujjwal K. Saha. "Influence of blade profiles on Savonius rotor performance: Numerical simulation and experimental validation." *Energy Conversion and Management* 186 (2019): 267-277. https://doi.org/10.1016/j.enconman.2019.02.058

[47] Saeed, Ramiz Ibraheem, Ahmed Al-Manea, Ahmed Khalid Ibrahim, and Dendy Adanta. "Numerical Investigation on the Effect of Profile and Blade Numbers in a Savonius Vertical Axis Wind Turbine." *CFD Letters* 14, no. 9 (2022): 75-88. https://doi.org/10.37934/cfdl.14.9.7588